JOURNAL OF PROPULSION AND POWER
Vol. 11, No. 2, March–April 1995

Particle Dynamics Simulations in Inlet Separator with an Experimentally Based Bounce Model

A. Hamed,* Y. D. Jun,† and J. J. Yeuan‡
University of Cincinnati, Cincinnati, Ohio 45221

This article presents a probabilistic simulation methodology for the particle dynamics through a helicopter engine's inlet separator with an experimentally based particle bounce model. The flowfield is determined from the numerical solution of the compressible Navier–Stokes equations with a two-equation turbulence model. The probabilistic simulations of the particle dynamics take into consideration the experimentally measured variance in the particle bounce conditions after surface interactions. Results are presented for the particle trajectories through the inlet and for the separator effectiveness over a range of sand particle sizes, and also for C-spec. sand.

Nomenclature

C_D = particle drag coefficient
D_p = particle diameter
F = aerodynamic force of interaction per unit mass of particles
r = radial coordinate
V = velocity
z = axial coordinate
β = angle between the particle velocity vector and the tangent to the surface
θ = circumferential coordinate
ρ = gas density
τ = time

Subscripts
p = particle
r = component in radial direction
z = component in axial direction
θ = component in circumferential direction
1 = particle condition before the impact
2 = particle condition after the impact

Introduction

INERTIAL-TYPE inlet particle separators (IPS) are used in helicopter engines to accomplish effective particle separation without sacrificing the aerodynamic performance. They feature highly contoured walls that result in complex flowfields within the core and scavenged flow passages. The simulations of the gas-particle dynamics require appropriate models for the interactions between the particles and the air, and between the particles and the solid boundaries. The accuracy of the predicted inlet separator efficiency is directly affected by these models. The particle trajectories in inlet separators have been studied.[1–5] In these investigations, the particle trajectory simulations were performed in the flowfield obtained from the numerical solution to the inviscid flow equations. Recently, Mann and Tan[6] demonstrated a difference in the separation efficiency for the relatively small particles (under 100 μm) when determined from the particle trajectories in the viscous flowfield. While the smaller particle trajectories are strongly influenced by the flowfield, larger particle trajectories are dominated by their inertia. Due to their higher inertia, the trajectories of these larger particles deviate more from the flow streamlines, and are mostly influenced by the surface impacts. After impacting a solid surface, the rest of a particle trajectory is determined by its rebounding conditions. The fidelity of the particle bounce model in representing the actual restitution characteristics after the surface impacts is therefore critical to the accurate simulation of the larger particle trajectories.

Experimental investigations of particle-bounce[7–9] were conducted in connection with the study of the material erosion due to particle impacts and with the particle trajectory simulations.[8] They involve measurements of the particle velocity components before impacting and after the bouncing from a target sample placed in a specially designed gas-particle flow tunnel. The nonintrusive laser Doppler velocimeter measurements at given test conditions indicate a variance in the particle rebounding conditions that can be represented in the form of probability density or cumulative distribution functions.[9] These type of tests are usually conducted for the selected particle-target material combination over a range of impact velocities and impingement angles.[8]

While the variance in particle rebounding conditions have long been reported by the experimentalists, deterministic methods continued to be used in the particle trajectory simulations based on experimentally measured mean values of the particle bounce conditions. In these deterministic simulations, the experimentally measured variance in the particle restitution characteristics is not represented, and the particle initial conditions uniquely determines their trajectories in the flowfield and their surface impacts. Hamed[10–12] implemented probabilistic methods in the particle trajectory simulations to model the variance in the particles shape and initial conditions,[10] and used the fast probability integral methods to explore the influence of variance in the particle bounce conditions in turbomachines.[11] Recently, Hamed and Kuhn[12] presented a probabilistic approach in which direct numerical simulations are used to model the experimentally measured variance in the particle restitution characteristics in the particle trajectory computations in gas turbines. The results of that study indicate that the predicted particle trajectories and surface erosion are sensitive to the particle bounce model.

The purpose of the present study is to investigate the particle dynamics in the inertial inlet particle separator with an

Presented as Paper 93-2156 at the AIAA/SAE/ASME/ASEE 29th Joint Propulsion Conference and Exhibit, Monterey, CA, June 28–30, 1993; received Oct. 30, 1993; revision received June 9, 1994; accepted for publication June 14, 1994.

*Professor, Department of Aerospace Engineering and Engineering Mechanics. Fellow AIAA.
†Research Assistant, Department of Aerospace Engineering and Engineering Mechanics. Student Member AIAA.
‡Postdoctoral Assistant, Department of Aerospace Engineering and Engineering Mechanics. Member AIAA.

experimentally based probabilistic particle bounce model, to simulate the observed variance in the actual measurements of the particle restitution characteristics. The Navier-Stokes equations with a two-equation k-ε turbulence model are solved in the axisymmetric flowfield simulations, and a three-dimensional particle trajectory code is used for the study of the particle dynamics. The particle trajectory simulations are conducted in a probabilistic structure and the results are compared with those obtained using a deterministic restitution model based on the mean values of the experimentally measured particle rebound conditions.

Methodology

The dynamics of suspended solid particles in internal flowfields are determined by the particle inertia and by the interactions between the gas and particles, and between the two phases and solid boundaries. For low particle concentrations, the effects of particle-particle interactions are not significant, and the gas flowfield is not affected by the presence of the particles. In the present study the gas flowfield is determined from the numerical solution to the compressible Navier-Stokes equations with a two equation k-ε turbulence model. Assuming that the flow is unaffected by the particles, the particle dynamics in the gas flowfield are determined from the numerical integration of the equations governing the particle's motion under the influence of their own inertia, and the aerodynamic forces due to the differences between the particle and gas velocities. An experimentally-based particle bounce model is used to determine the rebounding conditions after each surface impact in the probabilistic particle trajectory simulations.

Inlet Flowfield Simulations

The inlet flowfield simulations are based on the implicit solution of the compressible Navier-Stokes equations in strong conservation form and general curvilinear coordinates. The PARC code[13] with a two-equation k-ε turbulence model[14] was used in the computations of the flowfield. This code has been used extensively in supersonic inlet flowfield simulations,[15-17] and the computed results were compared with the experimental data.[17] In addition, we have also conducted a detailed comparative study[18] to assess the performance of the PARC code with both algebraic and two-equation turbulence model to three other codes with four different turbulence models in shock wave boundary-layer interactions. Based on comparisons with experimental results, the performance of the PARC code with the two-equation turbulence model was found to be very satisfactory under the severe adverse pressure gradients involved in the tested flowfield.[19]

Particle Dynamics Simulations

For the dilute particle concentrations in the inlet flowfield, the interparticle interactions are neglected. In addition, under the prevailing flow conditions in the inlet separator, the forces to accelerate the apparent mass of the particle as well as the forces on the particle due to flow pressure gradient and magnus effects are small compared to the aerodynamic drag force.

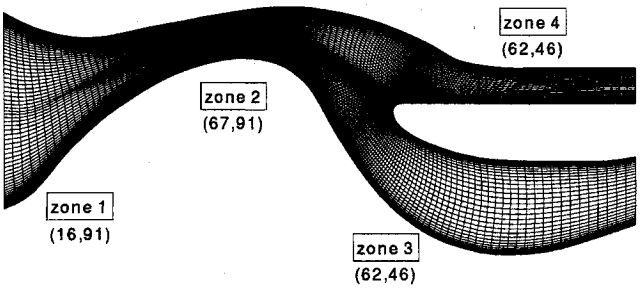

Fig. 1 Computational grid for an inertial particle separator.

The equations governing the particle motion are written in cylindrical polar coordinates as follows[8]:

$$\frac{d^2r_p}{d\tau^2} = F\left(V_r - \frac{dr_p}{d\tau}\right) + r\left(\frac{d\theta_p}{d\tau}\right)^2 \tag{1}$$

$$\frac{d^2\theta_p}{d\tau^2} = F\left(V_\theta - r\frac{d\theta_p}{d\tau}\right) - 2\frac{dr_p}{d\tau}\frac{d\theta_p}{d\tau} \tag{2}$$

$$\frac{d^2z_p}{d\tau^2} = F\left(V_z - \frac{dz_p}{d\tau}\right) \tag{3}$$

where r_p, θ_p, and z_p define the particle location in cylindrical polar coordinates, and V_r, V_θ, V_z represent the gas velocity components in the radial, circumferential, and axial directions, respectively. The last terms on the right side of Eqs. (1) and (2) represent the centrifugal force and Coriolis acceleration. The force of interaction between the two phases per unit mass of particles is represented by the first term on the right side of Eqs. (1–3). It is dependent on the relative velocity between the particles and the gas flow, as well as the particle size and shape

$$F = \frac{3}{4}\frac{\rho}{\rho_p}\frac{C_D}{D_p}\left[\left(V_r - \frac{dr_p}{d\tau}\right)^2 + \left(V_\theta - \frac{d\theta_p}{d\tau}\right)^2 + \left(V_z - \frac{dz_p}{d\tau}\right)^2\right]^{1/2} \tag{4}$$

where ρ and ρ_p are the gas and solid particle densities, re-

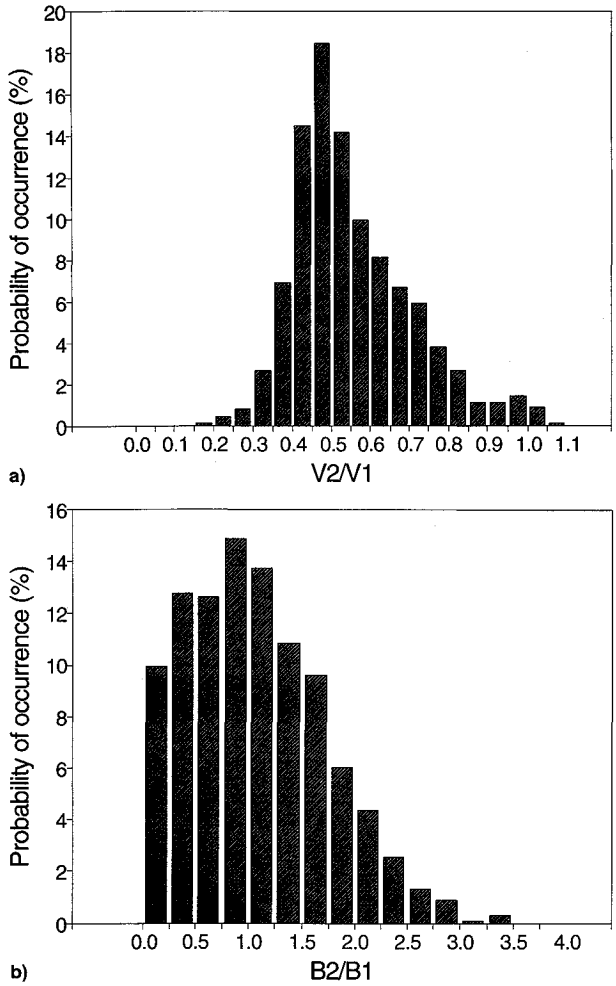

Fig. 2 Particle bounce characteristics for sand particles impacting Al 2024 target sample at 15-deg impingement angle: a) total velocity and b) directional restitution ratios.

spectively. The drag coefficient is a function of the Reynolds number, which is based on the relative velocity between the particle and the gas. Empirical relations[8] are used to fit the drag curve over a wide range of Reynolds numbers.

The numerical solution to the particle equations of motion is based on a fourth-order Runge-Kutta method, where the gas flow velocity and density are interpolated within the solution grid of Fig. 1. The particle dynamic simulations consist of the numerical integration of Eqs. (1–3) in the viscous inlet flowfield. Each trajectory is uniquely determined by the initial conditions until a particle impacts a solid boundary. The rest of the trajectory after a surface impact is determined by the probabilistic particle bounce conditions that constitute new initial conditions in the numerical integration of Eqs. (1–3).

Experimental Particle Bounce Characteristics

The experimental measurements of particle bounce characteristics were obtained using a 5-W argon-ion laser Doppler velocimeter in a specially designed tunnel.[8,9] The synchronized LDV measurements of the velocity components of the rebounding particles after impacting a sample target were obtained at different incoming conditions. Two experimentally-based particle restitution ratios (ratio between the rebounding and incoming conditions) are used to characterize the particle surface interactions for a given target sample under certain impacting conditions. Typical experimentally determined bounce characteristics for sand particles impacting target sample at 15-deg impingement angle are presented in Fig. 2. The experimentally observed variance in the particle bounce characteristics for a given test condition could not be characterized by a typical theoretical distribution (e.g., normal, log normal, etc.). The experimentally determined particle bounce characteristics, their mean values ± standard deviations over the range of tested impact angles (15–80 deg) are presented in Fig. 3.

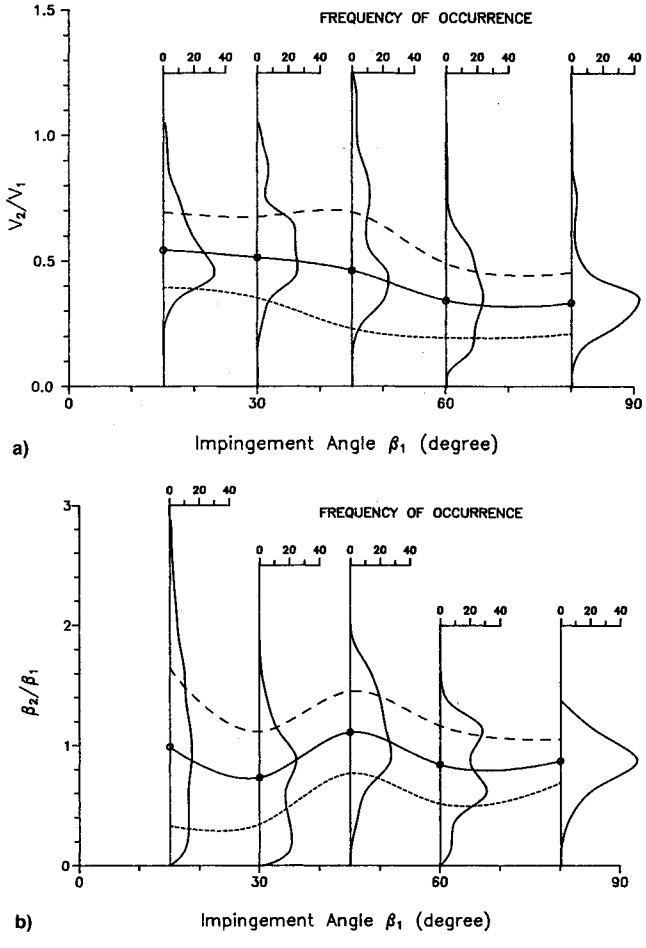

Fig. 3 Variation of restitution ratios with impingement angle: a) total velocity and b) directional restitution ratios.

Particle Bounce Model

A probabilistic approach was adopted in the particle trajectory code to simulate the experimentally measured variance in the particle bounce characteristics. Based on a randomly selected common probability for each simulated particle surface impact, the probabilistic bounce model determines the inverse cumulative distribution function (CDF) from the experimental results at all the tested impingement angles. These values are then spline-fitted to produce the rebounding particle conditions for that particular impact at the predetermined impingement angle. In this probabilistic modeling structure the particle rebounding conditions are dependent on the particle impacting conditions as well as the sampling probability. The outlined probabilistic bounce model significantly improves the accuracy of the particle trajectory predictions through the simulation of the experimentally measured variance in the particle bounce characteristics without affecting the efficiency and robustness. For a more detailed description of the probabilistic model and sampling methods, the reader can consult Ref. 12.

Results and Discussions

Figure 1 shows the grid structure for the flowfield solution in Allison's advanced IPS configuration 1.[19] Referring to Fig. 1, a total of 13, 257 grid points were used in the flowfield discretization with 16 × 91 and 67 × 91 grids in the entrance and midsection, and 62 × 46 grids in each of the core and scavenger flow passages. The y^+ value of the near-wall grid point was less than 2.0, with at least 15 grid points in the boundary layer in all regions. In performing the viscous flowfield simulations, the mass flow distribution between the core and the scavenger was controlled by changing the specified pressures at the two exits. The computations required 11,000 local time steps at 0.8 CFL number to reach steady-state solution based on six orders of magnitude reductions in the averaged rms error of the flux.

Figures 4–6 present the results of the viscous flowfield computations at a mass flow rate of 3.23 kg/s (7.11 lb/s), with 24% scavenge flow. The velocity vectors in Fig. 4 indicate a large recirculating flow region inside the scavenger passage near the splitter leading edge. Constant pressure (Fig. 5) and very low Mach numbers (Fig. 6) can be observed at the shroud in the same region. The pressure loss for the core and scavenge flow was determined to be 1.731 and 2.983%, respectively.

Particle Trajectories

Figures 7–10 present typical trajectories for selected sand particle sizes, whose material density is 2444 kg/m^3. The results in these figures were obtained for initial particle velocities equal to the local air velocity at the intake where the particles were evenly distributed in the radial direction. One can see that the small particles, up to 10 μm in diam, do not

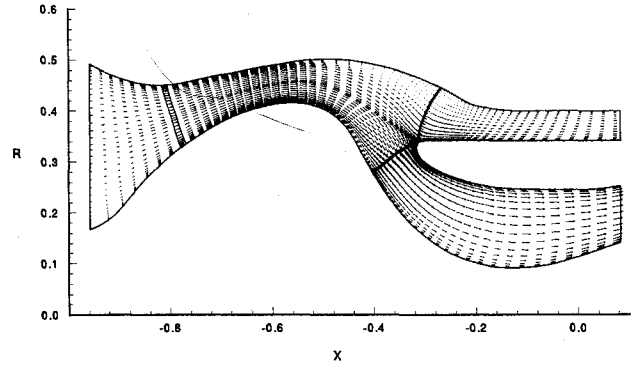

Fig. 4 Flow velocity vector plot for an inertial particle separator.

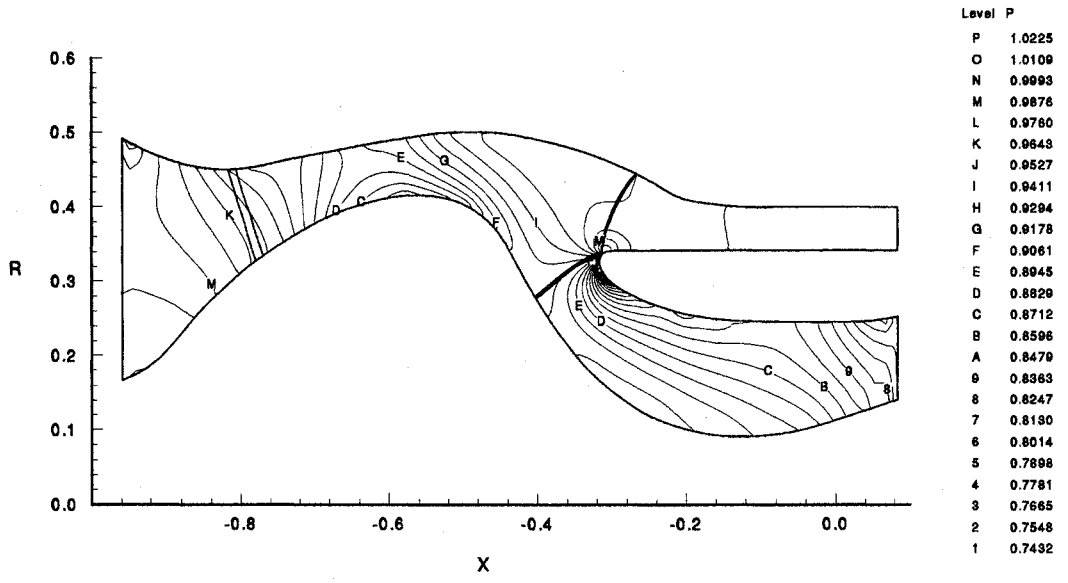

Fig. 5 Pressure contours for an inertial particle separator.

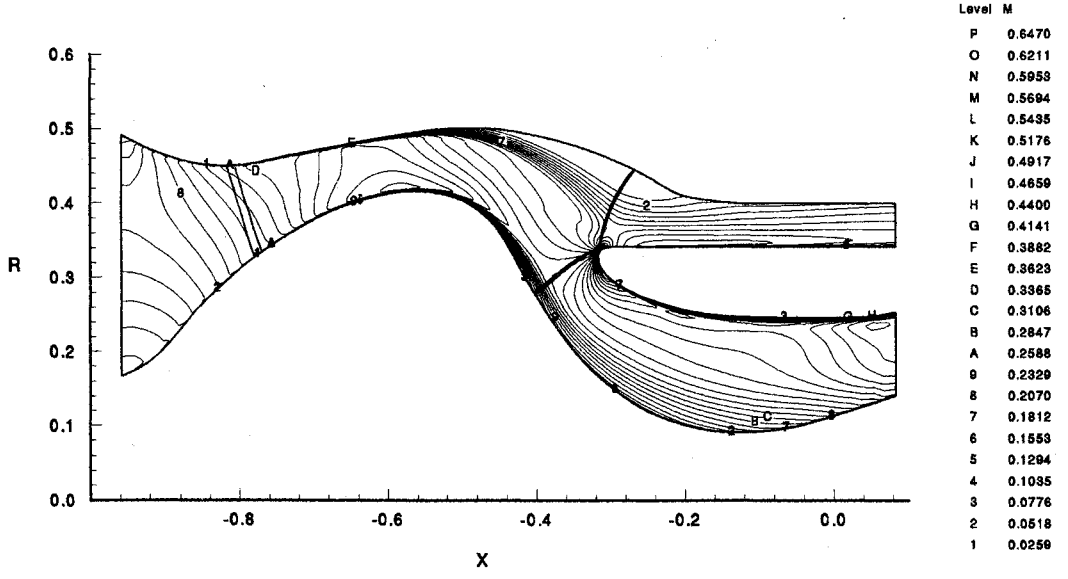

Fig. 6 Mach number contours for an inertial particle separator.

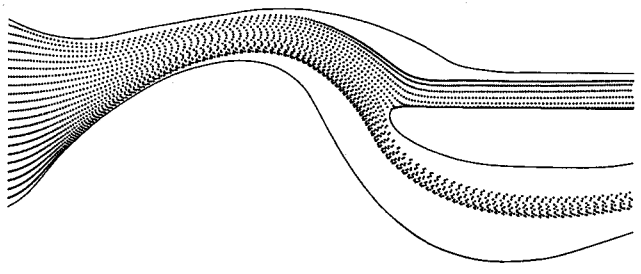

Fig. 7 Sample trajectories for 3-μm sand particles.

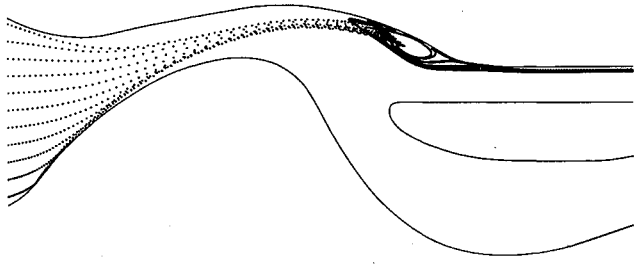

Fig. 8 Sample trajectories for 10-μm sand particles.

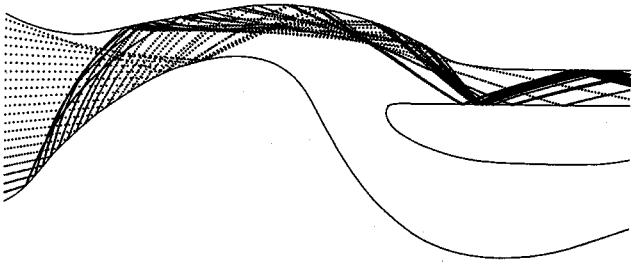

Fig. 9 Sample trajectories for 200-μm sand particles (deterministic bounce model).

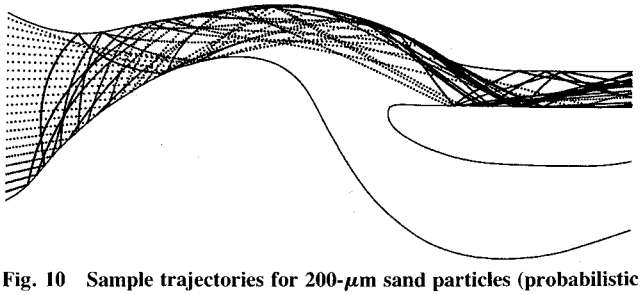

Fig. 10 Sample trajectories for 200-μm sand particles (probabilistic bounce model).

impact the boundaries except for the centerbody near the entrance and the splitter outer portion, and that a large percentage of the 3-μm particles is ingested into the engine core. Figure 8 indicates that most of the 10-μm particles are captured in the scavenger's recirculation region; a phenomenon observed for particles ranging between 5–20 μm in diam. Figures 9 and 10 present sample particle trajectories for 200-μm-diam particles obtained from simulations using deterministic and probabilistic particle bounce models. One can observe that most of these large particles repeatedly impact the inlet separator's surface. The trajectories obtained with the deterministic bounce model are based on the mean value of the experimentally measured particle restitution characteristics (Fig. 3). Comparing Figs. 9 and 10, one can see that the simulated variance in the particle bouncing conditions lead to more spread in the trajectories after the surface impacts.

Statistical assessment of the probabilistic trajectory simulations was conducted for 200-μm-diam particles to investigate the effects of sample size, and the seed for generating the random numbers used in specifying the particle initial conditions. Figures 11 and 12 present comparisons of the experimentally measured bounce condition at 15-deg impact angle, and those determined in the probabilistic particle trajectories for impact angles ranging between 13–17 deg. The comparison that was conducted for two sample sizes of 5000 and 1000 particle trajectories indicates very good agreement in the simulated statistical distributions of both total velocity and directional restitution ratios with the experimental data for both sample sizes. According to this assessment, one can conclude that a sample size of 5000 reproduces the experimentally measured variance with sufficient fidelity.

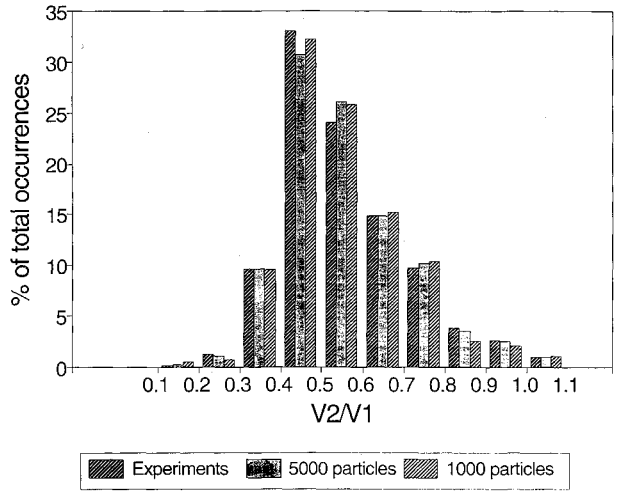

Fig. 11 Statistical assessment of particle trajectory sample size effect on simulated bounce velocity.

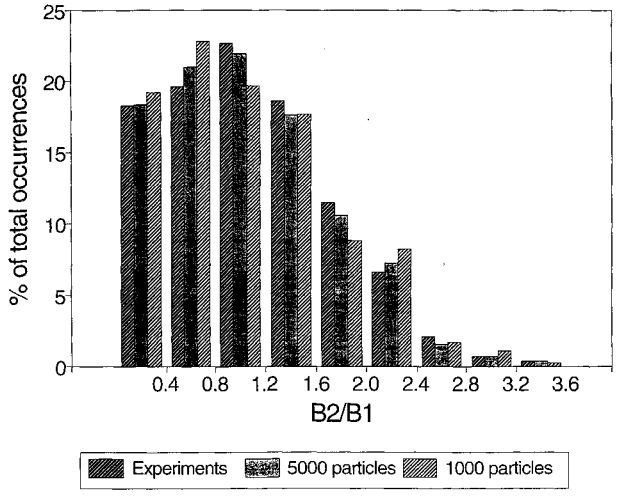

Fig. 12 Statistical assessment of particle trajectory sample size effect on simulated bounce angle.

Separator Efficiency

The inlet separator efficiency is defined as the ratio of the weight flow rate of the sand through the scavenger to the weight flow rate of sand at the entrance to the inlet. For the inlet separator efficiency investigation, trajectories were simulated for a large number of particles. In these simulations, the particles initial conditions were specified according to a probabilistic distribution model in which the particles were radially distributed in proportion to the mass flow, and were introduced with initial velocities between 50–100% of the local air velocity.

Figure 13 shows the influence of particle trajectory sample size on the separator efficiency for two different seed numbers (-85 and -200), which are used in the random number generator for the particles initial radial location. According to Fig. 13, the difference in the predicted separator efficiency is less than 0.5% for the two selected seed numbers at a sample size of 5000 particle trajectories. Similar assessments were also conducted for the different particle sizes (200, 300, and 400 μm), with three different sets of seed numbers used in the experimentally based bounce model.

A sample size of 5000 particles was used in the rest of the simulations for predicting the separator efficiency over the range of particle sizes. The results of these investigations with both deterministic and the probabilistic bounce models are presented in Fig. 14. One can see that the separator efficiency for the smaller particles up to 10 μm are basically unaffected by the bounce model, since their trajectories are dominated by the aerodynamic force of interaction between the particles and the flowfield. However, for particles greater than 20 μm

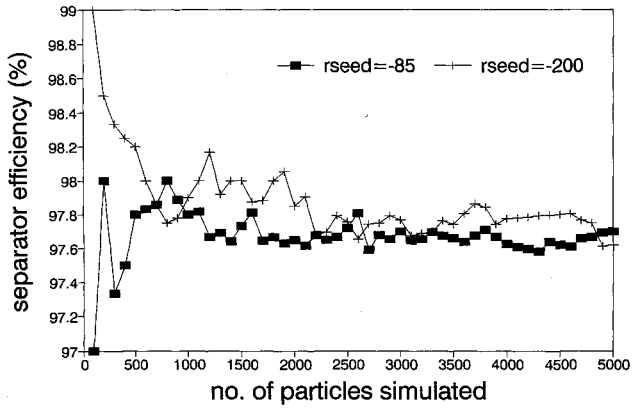

Fig. 13 Statistical assessment of sample size effect on the separator efficiency for two seed numbers.

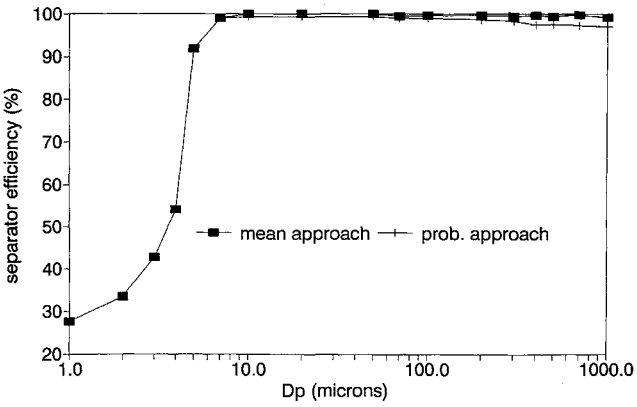

Fig. 14 Separator efficiency for different particle sizes.

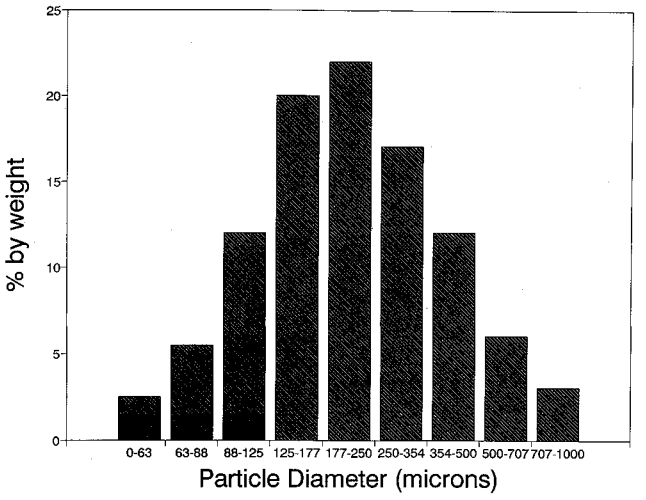

Fig. 15 C-spec. sand particle size distribution.

in diameter, the deterministic trajectory predictions overestimate the inlet separator efficiency and predict very little change in the separator efficiency with the particle size. On the other hand, the probabilistic model predictions indicate reduction in the efficiency as the particle size increases, reaching 3% for the 1000-μm particles.

Trajectory simulations through the inlet separator were conducted for C-spec. sand whose particle size distribution by weight is presented in Fig. 15. Based on the trajectory results for the specified particle size distribution, the deterministic bounce model leads to particle separator efficiency of 99.53% by weight. On the other hand, the trajectory simulations with the probabilistic bounce model resulted in a separator efficiency of 98.15% by weight. These findings indicate that the deterministic particle trajectory simulations overestimate the efficiency of the inertial inlet separator. In all reported particle trajectory simulations, the increase in CPU time for the probabilistic experimentally based bounce model did not exceed 10% that of the deterministic model.

Conclusions

Particle dynamics in an inlet particle separator were numerically simulated using a probabilistic approach with an experimentally based bounce model. According to the presented results, the effect of the variances in the particle bounce characteristics after their impacts with the solid surface can be significant for the larger particles. The predicted separator efficiency for C-spec. sand with a probabilistic bounce model was found to be lower by 1.4% than that with a deterministic model based on the mean bounce conditions. The improved accuracy in simulating the experimentally measured variance in the particle bounce conditions after surface impacts is accomplished at the same level of efficiency and robustness as the deterministic model based on the experimental mean values.

Acknowledgments

This work was supported by NSF Grant CTS-901239, M. Rocco, Project Monitor, Washington, DC. The flowfield computations were performed on the Cray Y-MP of the Ohio Super Computer, Columbus, Ohio. The authors wish to thank B. Vittal of Allison Gas Turbine Division, GMC, for providing the inlet separator geometry.

References

[1]Hamed, A., "Particle Dynamics of Inlet Flowfields with Swirling Vanes," *Journal of Aircraft*, Vol. 19, No. 9, 1982, pp. 707–712.

[2]Hamed, A., "Solid Particle Dynamic Behavior Through Twisted Blade Rows," *Journal of Fluids Engineering*, Vol. 106, Sept. 1984, pp. 251–256.

[3]Breitman, D. S., Dueck, E. G., and Habashi, W. G., "Analysis of a Split Flow Inertial Particle Separator Using Finite Elements," *Journal of Aircraft*, Vol. 22, No. 2, 1985, pp. 135–140.

[4]Vittal, B. V. R., Tipton, D. L., and Bennett, W. A., "Development of an Advanced Vaneless Inlet Particle Separator for Helicopter Engines," AIAA Paper 85-1277, July 1985.

[5]Kim, J. J., Breer, M. D., Gass, J., and Kneeling, D., "Sand Separator Efficiency Calculation for the JVX Tilt Rotor Aircraft Inlet," June 1986.

[6]Mann, D. L., and Tan, S. C., "A Theoretical Approach to Particle Separator Design," Ninth International Symposium on Air Breathing Engines, Vol. 2, International Society for Air Breathing Engines, ISOABE 89-7084, Sept. 1989, pp. 801–806.

[7]Tabakoff, W., "Measurements of Particles Rebound Characteristics on Materials Used in Gas Turbines," *Journal of Propulsion and Power*, Vol. 7, No. 5, 1991, pp. 805–813.

[8]Hamed, A., Tabakoff, W., and Wenglarz, R., "Particulate Flow, Blade Erosion and Performance Deterioration," von Kármán Inst. for Fluid Dynamics, von Kármán Lecture Series 1988–89, Brüssels, Belgium, May 1988.

[9]Hamed, A., and Tabakoff, W., "Experimental Investigation of Particle Surface Interactions for Turbomachinery Applications," *Laser Anemometry Advances and Applications*, Vol. 2, American Society of Mechanical Engineers, *Proceedings of the 4th International Conference on Laser Anemometry, Advances and Applications* (Cleveland, OH), 1991, pp. 775–780.

[10]Hamed, A., and Moy, H., "Probabilistic Simulation of Fragment Dynamics and Their Surface Impacts in the SSME Turbopump," *First ASME-JSME Fluids Engineering Conference*, ASME FED-Vol. 120 (Portland, OR), June 1991, pp. 141–150.

[11]Hamed, A., "An Investigation in the Variance in Particle Surface Interactions and Their Effects in Gas Turbines," *Journal of Engineering of Gas Turbines and Power*, Vol. 114, April 1992, pp. 235–241.

[12]Hamed, A., and Kuhn, T., "Effects of Variational Particle Restitution Characteristics on Turbomachinery Erosion," American Society of Mechanical Engineers Paper 93-GT-124, May 1993.

[13]Cooper, G. K., and Sirbaugh, J. R., "PARC Code: Theory and Usage," Arnold Engineering Development Center, AEDC-TR-89-15, Arnold Air Force Base, TN, Dec. 1989.

[14]Nichols, R. H., "A Two-Equation Model for Compressible Flows," AIAA Paper 90-0494, Jan. 1990.

[15]Saunders, J. D., and Keith, T. G., Jr., "Results from Computational Analysis of a Mixed Compression Supersonic Inlet," AIAA Paper 91-2581, June 1991.

[16]Reddy, D. R., Benson, T. J., and Weir, L. J., "Comparison of 3-D Viscous Flow Computations of Mach 5 Inlet with Experimental Data," AIAA Paper 90-0600, Jan. 1990.

[17]Weir, L. J., Reddy, D. R., and Rupp, G. D., "Mach 5 Inlet CFD and Experimental Results," AIAA Paper 89-2355, July 1989.

[18]Hamed, A., "An Investigation of Oblique Shock/Boundary Layer Interaction Control," Air Force Office of Scientific Research TR Contract 91-0101, Univ. of Cincinnati, Cincinnati, OH, Jan. 1992.

[19]Vittal, B., private communication, Indianapolis, IN, 1992.